

BRIGHTNESS AND COHERENCE OF RADIATION FROM UNDULATORS AND HIGH-GAIN FREE ELECTRON LASERS

Kwang-Je Kim

Lawrence Berkeley Laboratory
University of California
Berkeley, California 94720

1. Introduction

Undulators in next-generation, low-emittance electron storage rings^{1,2,3} are sources of extremely bright radiation in wide range of spectral region covering photon energies between several eV to several tens of keV. The expected brightness is several times 10^{19} photons per second per (mm-mrad)² per 0.1% bandwidth. Furthermore, the undulator radiation from storage rings of moderate energies, between 1 to 2 GeV, will have substantial coherence properties in the vacuum ultraviolet and the soft x-ray regions, generating tens of milliwatts of time-averaged coherent power of 1-micron coherence length.⁴ At the same time, free-electron lasers⁵ (FELs), which have been so far limited to the infrared and visible wavelengths, will eventually be developed to generate even more intense and coherent radiation for the vacuum ultraviolet and shorter wavelengths. Among different FEL schemes,⁶ the so-called high-gain FELs^{7,8} are conceptually the most straightforward extension of the undulator techniques, the transition to high-gain FELs occurring simply with better electron beam qualities and longer undulators. High-gain FELs can produce tens of megawatts of peak coherent power at wavelengths shorter than 1000 Å. With these in mind, the purpose of this paper is to review the radiation characteristics of undulators and high-gain FELs.

The angular distribution and the intensity characteristics of synchrotron radiation are well understood and extensively reviewed in the literature.^{9,10} In order to properly discuss brightness and coherence, however, it is necessary to utilize the phase-space description^{11,12} which is perhaps less widely understood. In this paper, we give a rigorous foundation of phase-space description in terms of the Wigner distribution function.¹³ The phase-space description allows us to describe systematically how the radiation propagates through optical medium and how it forms images and interference pattern. Also, it provides a convenient basis to discuss the effects of electron beam emittance on radiation characteristics. The flux density in phase-space is called the brightness, which is invariant under optical transformation and therefore is a true characterization of the source strength. The photon flux contained in a phase space area given by $\lambda/2$, where λ is the wavelength, is transversely coherent.

For synchrotron radiation, the brightness can be explicitly calculated. Taking into account the effects of electron-beam emittance, it is found that the brightness is given by a convolution of the single-electron brightness and the probability distribution function of electrons in the emittance phase space.^{11,14} This remarkable result is referred to as the brightness convolution theorem. The final expression for the undulator brightness is rather complicated, but the important features can be understood with suitable approximation.

The evolution of radiation characteristics and the electron correlation from simple undulators to high-gain FELs can be determined by solving the Maxwell-Klimontovich equations.¹⁵ The solution of these equations make it clear how electron correlation develops with concomitant build-up of radiation intensity. The radiation in the high-gain regime exhibits exponential growth and guiding, and is fully coherent transversely.

Section 2 is an introduction to the phase-space method in wave optics and synchrotron radiation. In Section 3, coherence is discussed from the phase-space point of view. The method is applied to the undulator radiation in Section 4. Section 5 contains discussions of undulator performances in next-generation synchrotron radiation facility. Finally we discuss in Section 6 the characteristics of the high-gain FELs and their performances.

2. Phase Space and Brightness

In discussing the propagation properties of radiation, the density of the photon flux in phase-space plays a fundamental role and is generally referred to in optics as the brightness.¹⁶ (It should be noted that this quantity is sometimes called brilliance.) The brightness \mathcal{B} is the phase-space density of the photon flux \mathcal{F} , as follows:

$$\mathcal{B}(\mathbf{x}, \phi, z) = \frac{d^4 \mathcal{F}}{d^2 \mathbf{x} d^2 \phi} \quad (1)$$

Here $\mathbf{x} = (x, y)$, where x and y are respectively the horizontal and vertical coordinates in a plane transverse to the optical axis and $\phi = (\phi, \psi)$, where ϕ and ψ are respectively the horizontal and vertical angles with respect to the optical axis. In the above, z is the coordinate along the optical axis.

The brightness has an unambiguous physical meaning in geometric optics as phase-space density of rays. The two-dimensional vectors \mathbf{x} and ϕ can be interpreted as the position and angle of a ray passing through the transverse plane. Propagation through optical medium composed of free space and lenses is described by the following linear coordinate transformation:

$$\mathcal{B}(\mathbf{x}, \phi, z_2) = \mathcal{B}(\mathbf{x}', \phi', z_1) \cdot \begin{pmatrix} \mathbf{x}' \\ \phi' \end{pmatrix} = M^{-1} \begin{pmatrix} \mathbf{x} \\ \phi \end{pmatrix} \quad (2)$$

Here M is a 2×2 matrix given by a product of matrices — one for each lens and free space. These matrices are given by

$$M_\ell = \begin{pmatrix} 1 & \ell \\ 0 & 1 \end{pmatrix} \quad \text{for a free space of length } \ell, \quad (3)$$

$$M_f = \begin{pmatrix} -1 & 0 \\ -1/f & 1 \end{pmatrix} \quad \text{for a lens of focal length } f.$$

These transformations are familiar from particle optics in accelerator physics.¹⁷ The simplicity of the transformation, Eq. (2), is the reason why the brightness is useful. In addition, the brightness at the phase-space origin, $\mathbf{x} = 0$ and $\phi = 0$, is invariant. That is, independent of z . Thus the brightness (evaluated at the phase-space origin) is a true characterization of the intrinsic source strength.

Integrating the brightness over the angles or position, we obtain the spatial or the angular density of flux:

$$A(\phi, z) \equiv \frac{d^2 \mathcal{F}}{d^2 \phi} = \int \mathcal{B}(\mathbf{x}, \phi, z) d^2 \mathbf{x}, \quad (4)$$

$$S(\mathbf{x}, z) \equiv \frac{d^2 \mathcal{F}}{d^2 \mathbf{x}} = \int \mathcal{B}(\mathbf{x}, \phi, z) d^2 \phi. \quad (5)$$

For synchrotron radiation, the angular density of flux [Eq. (4)] has traditionally been the most familiar quantity, as it can be calculated from standard textbook formulas, and it is sometimes mistakenly called brightness. However, it is not an invariant measure of the source strength. Finally, one obtains the flux by integration, as follows:

$$\mathcal{F} = \int \frac{d^2 \mathcal{F}}{d^2 \phi} d^2 \phi = \int \frac{d^2 \mathcal{F}}{d^2 \mathbf{x}} d^2 \mathbf{x}. \quad (6)$$

The flux is another invariant that characterizes the source strength.

It is generally convenient to consider the various differential fluxes introduced above in a small bandwidth around a given energy. In this case, we use the adjective *spectral*. Thus, we speak of the spectral brightness, spectral flux, the angular density of spectral flux, and so on.

(a) Brightness in Wave Optics

In wave optics, the brightness cannot be calculated as the density of rays, and a more fundamental approach is necessary. We start from the electric field $E(\mathbf{x}, z, t)$ and its Fourier transforms:

$$E_w(\mathbf{x}, z) = \frac{1}{\sqrt{2\pi}} \int E(\mathbf{x}, z, t) e^{i\omega t} dt \quad (7)$$

$$\mathcal{E}_w(\phi, z) = \frac{1}{\lambda^2} \int E_w(\mathbf{x}, z) e^{-ik\phi \cdot \mathbf{x}} d^2 \mathbf{x}, \quad (8)$$

where $k = 2\pi/\lambda = \omega/c$. The spectral brightness is then introduced as the following Wigner distribution function.¹¹

$$\begin{aligned} \mathcal{B}(\mathbf{x}, \phi, z) &= \frac{d\omega}{\hbar\omega} \frac{2\epsilon_0 c}{T} \int d^2\theta \langle \mathcal{E}_\omega^*(\phi + \theta/2, z) \mathcal{E}_\omega(\phi - \theta/2, z) \rangle e^{-ik\mathbf{x}\cdot\theta} , \\ &= \frac{d\omega}{\hbar\omega} \frac{2\epsilon_0 c}{T\lambda^2} \int d^2\xi \langle E_\omega^*(\mathbf{x} + \xi/2, z) E_\omega(\mathbf{x} - \xi/2, z) \rangle e^{ik\phi\cdot\xi} . \end{aligned} \quad (9)$$

The units throughout this paper are in MKS, and ϵ_0 = vacuum dielectric constant, \hbar = the Planck's constant/ 2π , c = velocity of light, and T is the duration of the electric field. The coefficient in Eq. (9) is such that $\mathcal{B}T$ is the total number of photons per unit time per unit phase-space area in the spectral bandwidth $d\omega$. The angular brackets represent a statistical average in case the field is random as is the case for undulator radiation by electron beams.

The brightness as defined by Eq. (9) is not positive definite and thus cannot by itself be interpreted as a flux density in physical phase space. However, one can show that the quantities A and S , obtained by integration through Eqs. (4) and (5), are positive definite and do indeed correspond to the genuine angular and spatial density of flux, respectively. Furthermore, the phase-space transformation property, Eq. (2), can also be shown to apply in the present case.¹¹ Thus we are justified in calling the quantity defined by Eq. (9) as the brightness.

The statement that the brightness transformation, Eq. (2), is the same both for the geometric and wave optics needs to be qualified when slits are present. For geometric optics, the effect of a slit is simply to remove those rays which end on the opaque parts of the slit. In wave optics, the brightness before the slit \mathcal{B}_i and after the slit \mathcal{B}_f are related by

$$\mathcal{B}_f(\mathbf{x}, \phi) = \int G(\mathbf{x}, \phi - \phi') \mathcal{B}_i(\mathbf{x}, \phi') d^2\phi' . \quad (10)$$

Here

$$G(\mathbf{x}, \phi) = \frac{1}{\lambda^2} \int d^2\xi S^*(\mathbf{x} + \xi/2) S(\mathbf{x} - \xi/2) e^{ik\phi\cdot\xi} .$$

The function $S(\mathbf{x})$, which varies between 0 and 1, is the slit transmittance. Equation (10) gives rise to the well-known diffraction patterns.

(b) Examples

As a simple example in wave optics, we consider the Gaussian mode of an optical resonator. Choosing $z = 0$ to be the location of the waist, and inserting the well-known expression¹⁸ for the electric field into Eq. (9), one obtains

$$\mathcal{B}(\mathbf{x}, \phi, z) = \frac{\mathcal{F}}{(\lambda/2)^2} \exp \left[-\frac{1}{2} \left[\frac{(\mathbf{x} - z\phi)^2}{\sigma_r^2} + \frac{\phi^2}{\sigma_r'^2} \right] \right] , \quad (11)$$

where \mathcal{F} is the total flux, σ_r and σ_r' are related to the more familiar quantities w_0 (waist) and Z_R (Rayleigh range) by $\sigma_r = w_0/2$ and $\sigma_r' = \sigma_r/Z_R$. These are related by $2\pi\sigma_r\sigma_r' = \lambda/2$.

The electron distribution in its physical phase space is an example of brightness in geometric optics. In the straight sections, the probability distribution of finding electrons with a transverse coordinate $\mathbf{x}_e = (x_e, y_e)$ and angle $\phi_e = (\phi_e, \psi_e)$ is

$$\begin{aligned} f(\mathbf{x}_e, \phi_e, z) &= \frac{1}{(2\pi)^2 \epsilon_x \epsilon_y} \exp \left[-\frac{1}{2} \left[\frac{(x_e - z\phi_e)^2}{\sigma_x^2} \right. \right. \\ &\quad \left. \left. + \frac{(y_e - z\psi_e)^2}{\sigma_y^2} + \frac{\psi_e^2}{\sigma_x'^2} + \frac{\phi_e^2}{\sigma_y'^2} \right] \right] . \end{aligned} \quad (12)$$

Here $\epsilon_x = \sigma_x \sigma_x'$ and $\epsilon_y = \sigma_y \sigma_y'$ are known as the emittances. The quantities corresponding to the Raleigh length, $\beta_x = \sigma_x/\sigma_x'$ and $\beta_y = \sigma_y/\sigma_y'$, are determined from the lattice configuration.

(c) Synchrotron Radiation and the Brightness Convolution Theorem

For synchrotron radiation, the single-electron brightness can be calculated explicitly starting from the radiation formula¹⁹

$$\mathcal{E}_\omega(\phi, z=0) = \frac{q}{4\pi\epsilon_0 c} \frac{\omega}{\lambda\sqrt{2\pi}} \int dt \mathbf{n} \times (\mathbf{n} \times \beta) e^{i\omega t - n\pi/c} . \quad (13)$$

Here, q = electron charge, βc and \mathbf{r} are respectively the velocity and position three-vectors of the electron trajectory, and $\mathbf{n} = (\phi, 1 - \phi^2/2)$ is the direction three-vectors. (The paraxial approximation,

$\sqrt{1 - \phi^2} \sim 1 - \phi^2/2$, is assumed throughout this paper.) In this paper, we consider only the dominant polarization component, usually in the horizontal direction. The RHS of Eq. (13) is therefore to be evaluated for the x -component.

The brightness for a collection of electrons is given by a sum over the individual contributions. Assuming that the orbit deviation of different electrons are small, and that the electrons are randomly distributed, one can show that the many-electron brightness \mathcal{B} is related to the brightness \mathcal{B}^0 from a single electron on the ideal orbit as follows:^{11,14}

$$\mathcal{B}(\mathbf{x}, \phi, z) = N_e \int \mathcal{B}^0(\mathbf{x} - \mathbf{x}_e, \phi - \phi_e, z) f(\mathbf{x}_e, \phi_e, z) d^2\mathbf{x}_e d^2\phi_e . \quad (14)$$

Here the function f is the probability density of electrons in its phase space (\mathbf{x}_e, ϕ_e) , Eq. (12). Equation (14) is remarkable because the brightness in wave optics combines with the brightness in geometric optics as if the former is also a genuine probability distribution.

3. Coherence

Another important characteristic of radiation is the coherence, which is the degree to which the radiation can exhibit interference patterns. Two types of coherence can be distinguished:²⁰ the transverse coherence refers to the coherence of the electromagnetic disturbances at two points on the transverse plane at a given time. The temporal coherence refers to the case of two points separated in time.

The temporal coherence is characterized by the coherence length ℓ_c over which the wave maintains a definite phase relationship. It is related to the bandwidth by

$$\ell_c = \lambda(\lambda/\Delta\lambda) = \lambda^2/\Delta\lambda \quad (15)$$

The transverse coherence is characterized by the transversely coherent flux $\mathcal{F}_{coh,T}$. This quantity can be determined from a simple thought experiment shown in Fig. 1 as the flux that goes into the area between the interference maxima and minima, for all different angles ϕ . One obtains (for this and next sections, we will be concerned with brightness and fields at the source plane $z=0$, and will therefore suppress the z -dependence.)

$$\begin{aligned} \mathcal{F}_{coh,T} &= \alpha \frac{d\omega}{\omega} \frac{1}{T} \int d^2\phi \left| \langle \mathcal{E}_\omega^*(-\phi) \mathcal{E}_\omega(\phi) \rangle \right| \\ &\geq (\lambda/2)^2 \mathcal{B}(0,0) \end{aligned} \quad (16)$$

In general, we may define the effective phase space area occupied by the radiation as $\Omega = \mathcal{F}/\mathcal{B}(0,0)$. Since $\mathcal{F}_{coh,T}$ is always less or equal to \mathcal{F} , the total flux, it follows from Eq. (16) that the effective phase-space area Ω cannot be smaller than $(\lambda/2)^2$. This is due to the wave nature of the radiation, and is to be compared with the case of geometrical optics where there is no restriction to the minimum size of the phase space area. Conversely, it also follows that when the phase-space area of an arbitrary radiation is $(\lambda/2)^2$, the radiation is fully coherent transversely. Thus, the phase-space method provides a very convenient criteria for the transverse coherence.

Under certain circumstances, for example when the source is symmetric so that $\mathcal{E}_\omega(\phi) = \mathcal{E}_\omega(-\phi)$, Eq. (16) becomes an equality:

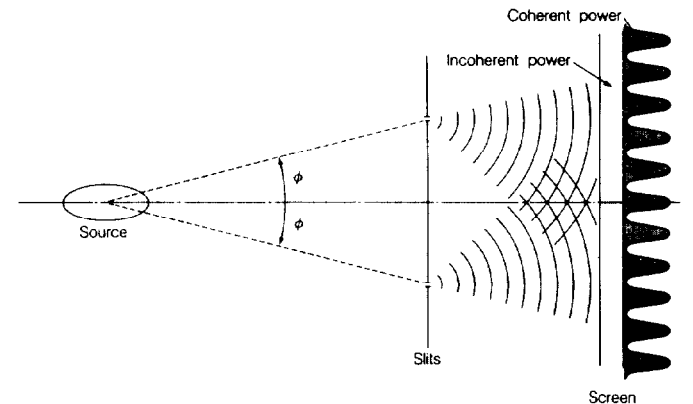


Fig. 1. A thought-experiment to determine the degree of the transverse coherence.

$$\mathcal{F} = (\lambda/2)^2 \mathcal{B}(0,0) . \quad (17)$$

This relation is easily checked for the case of the Gaussian mode, Eq. (11), and the fact that $\mathcal{F} = \mathcal{F}_{coh}$ for that case.

4. Phase-Space Characteristics of Undulator Radiation

The spectrum of undulator radiation is sharply peaked around $\omega \sim n\omega_1$, at odd harmonics around the fundamental frequency $\omega_1 = 2\pi c 2\gamma^2/\lambda_u(1+K^2/2)$, where γ = electron energy divided by its rest energy, λ_u = magnet period, $K = eB_0\lambda_u/2\pi mc$, B_0 = peak value of the magnetic field and m = the electron mass. Near the spectral peaks,

$$\omega/\omega_1 = n + \Delta\nu, \quad \Delta\nu \ll 1, \quad (18)$$

the electric field of an N -period undulator is approximately given by

$$\mathcal{E}_\omega(\phi) = \frac{q}{4\pi\epsilon_0 c} \frac{\lambda_u}{\lambda^2\sqrt{2\pi}} (-1)^{(N-1)n} \frac{K}{i\gamma} [JJ]_n \quad (19)$$

$$\frac{\sin\pi N(\Delta\nu + n\gamma^2\phi^2/(1+K^2/2))}{\pi(\Delta\nu + n\gamma^2\phi^2/(1+K^2/2))} .$$

Here n is an odd integer and

$$[JJ]_n = J_{\frac{n+1}{2}} \left[\frac{K^2 n}{4(1+K^2/2)} \right] - J_{\frac{n-1}{2}} \left[\frac{K^2 n}{4(1+K^2/2)} \right] . \quad (20)$$

Inserting Eq. (21) to Eq. (9), we obtain the following expression for the single-electron brightness:

$$\mathcal{B}^0(\mathbf{x}, \phi) = \mathcal{F}^0 \frac{1}{(\lambda/2)^2} \frac{1}{\pi C(\Delta\tilde{\nu})} \quad (21)$$

$$\int_{-1}^1 d\tilde{s} \int_0^{1-|\tilde{s}|} \frac{d\ell}{\ell} \sin \left[\frac{(\tilde{x} - \tilde{s}\tilde{\phi})^2}{\ell} - \ell(\tilde{\phi}^2 + 2\Delta\tilde{\nu}) \right] ,$$

where the superscript 0 refers to the single electron quantity, and we have used the following scaled variables:

$$\tilde{\phi} = \sqrt{kL/2} \phi, \quad \tilde{x} = \sqrt{2k/L} x, \quad \Delta\tilde{\nu} = \pi N \Delta\nu = \pi N(\omega/\omega_1 - n) . \quad (22)$$

The single-electron flux is given by

$$\mathcal{F}^0 = \frac{\alpha}{T} \frac{d\omega}{\omega} \gamma^2 \frac{n^2 K^2}{(1+K^2/2)} \frac{N}{2} [JJ]_n^2 C(\Delta\tilde{\nu}) . \quad (23)$$

The function C in Eqs. (21) and (23) is

$$C(\Delta\tilde{\nu}) = \frac{2}{\pi} \int_{\Delta\tilde{\nu}}^{\infty} \left[\frac{\sin x}{x} \right]^2 dx, \quad C(0) = 1 . \quad (24)$$

The integral in Eq. (21) is singular at $\mathbf{x} = \phi = 0$, so we define $\mathcal{B}^0(0,0)$ to be limiting value of $\mathcal{B}^0(\mathbf{x}, \phi)$ as \mathbf{x} and ϕ vanish from non-zero value. After a careful analysis, we find

$$\mathcal{B}^0(0,0) = \mathcal{F}^0/(\lambda/2)^2 . \quad (25)$$

This is to be expected from Eq. (17) since the single-electron flux is clearly coherent and the electric field given by Eq. (19) is symmetric in ϕ . Thus, the effective phase-space area Ω is $(\lambda/2)^2$ for all $\Delta\tilde{\nu}$.

Integrating Eq. (21), one obtains

$$A^0(\phi) = \int \mathcal{B}^0(\mathbf{x}, \phi) d^2\mathbf{x} = \mathcal{F}^0 \frac{L}{C(\Delta\tilde{\nu})\pi\lambda} \left[\frac{\sin(\Delta\tilde{\nu} + \tilde{\phi}^2/2)}{(\Delta\tilde{\nu} + \tilde{\phi}^2/2)} \right]^2, \quad (26)$$

$$S^0(\mathbf{x}) = \int \mathcal{B}^0(\mathbf{x}, \phi) d^2\phi \quad (27)$$

$$= \mathcal{F}^0 \frac{\pi}{C(\Delta\tilde{\nu})\lambda L} \left[\frac{2}{\pi} \int_{\tilde{x}}^{\infty} \frac{d\ell}{\ell} \sin \left[\frac{\ell}{2} - \frac{\Delta\tilde{\nu}\tilde{x}^2}{\ell} \right] \right]^2 .$$

These results can also be obtained directly from Eq. (19).

In Fig. 2, we show the shape of the brightness function, Eq. (21), evaluated at $\Delta\tilde{\nu} = 0$ for the case ϕ and \mathbf{x} are parallel to each other. The integration was made well-behaved by transforming the integration path in complex plane.²¹ The main feature of the Fig. 2 can be made plausible if we note that Eq. (21) is of the form

$$\mathcal{B}^0(\mathbf{x}, \phi) = \int_{-L/2}^{L/2} dz G(\mathbf{x} - z\phi, \phi, z) . \quad (28)$$

The quantity $G(\mathbf{x}, \phi, z) dz$ can be interpreted as the brightness due to the source element dz seen from the transverse plane at z . The brightness

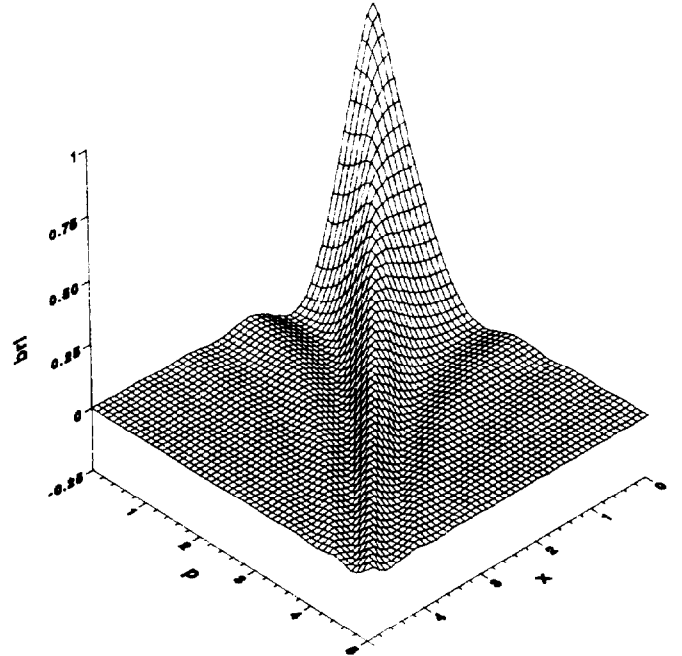


Fig. 2. The brightness function normalized unity at origin. \mathbf{x} and ϕ correspond respectively to the normalized variables \tilde{x} and $\tilde{\phi}$ in the text.

seen from the plane at $z = 0$ is obtained by replacing the variable \mathbf{x} by $\mathbf{x} - z\phi$ (see Eq. (2)). This is the depth-of-field effect in wave optics and is apparent in Fig. (2).

We attempt the following approximation for G :

$$G(\mathbf{x}, \phi, z) = \frac{\mathcal{F}^0}{(2\pi\sigma_r\sigma_r')^2} g(z) \exp \left[-\frac{1}{2} \left(\frac{x^2}{\sigma_r^2} + \frac{\phi^2}{\sigma_r'^2} \right) \right] . \quad (29)$$

If we set $g(z) = \delta(z)$, the brightness function takes the form of the Gaussian mode in laser resonator, Eq. (11) evaluated at $z = 0$. Such a model is helpful in studying the main features of the phase-space characteristics of undulator radiation.^{11,22} However, the model is perhaps too crude; for example, it does not take into account the depth-of-field effect. For a better approximation, we shall determine the parameters σ_r and σ_r' , and the function $g(z)$ by requiring that Eq. (25), Eq. (26) at $\phi = 0$, and Eq. (27) at $\mathbf{x} = 0$ are satisfied, and that the total flux obtained by integration reproduces \mathcal{F} . We also set $\Delta\nu = 0$ for this approximation. With the choice $\sigma_r = \sqrt{2\lambda L}/4\pi$, $\sigma_r' = \sqrt{\lambda/2L}$, and $g(z) = (1 + \sigma_r^2 z^2/\sigma_r'^2)/4L$, all of the above requirements are exactly satisfied except the last one which is satisfied with 7% error.

To take into account the emittance of the electron beam, we use the brightness convolution theorem, Eq. (14). Assuming that the electron distribution is given by Eq. (12), we obtain for the peak brightness

$$\mathcal{B}(0,0) = \mathcal{F} \int dz g(z) / \left(\Omega_x(z^2) \Omega_y(z^2) \right) , \quad (30)$$

where $\mathcal{F} = N_e \mathcal{F}^0$ is the N_e -electron flux,

$$\Omega_x(z^2) = 2\pi \sqrt{(\sigma_x^2 + \sigma_x'^2)(\sigma_x^2 + \sigma_x'^2 + z^2\sigma_x^2\sigma_x'^2)} , \quad (31)$$

and similarly for $\Omega_y(z^2)$. Here σ_x (σ_y) and σ_x' (σ_y') are respectively the rms beam size and angular divergence in the x (y) direction. Equation (30) can be written as $\mathcal{B}(0,0) = \mathcal{F}/\bar{\Omega}_x \bar{\Omega}_y$, where the effective phase-space areas $\bar{\Omega}_x$ and $\bar{\Omega}_y$ are obtained by replacing z^2 in Eq. (30) its average \bar{z}^2 , the precise meaning of the average being specified by Eq. (30). The phase-space area increases from the coherent phase-space area $\lambda/2$ (in each dimension) by electron-beam effects and depth-of-field effects. For a given value of emittance $\epsilon_x = \sigma_x\sigma_x'$, and $\epsilon_y = \sigma_y\sigma_y'$, the phase-space area is minimized when

$$\beta_x = \beta_y = \sqrt{\bar{z}^2 + (L/2\pi)^2} . \quad (32)$$

Taking \bar{z}^2 to be about $(L/2)^2/2$, this leads to $\beta_x = \beta_y \sim 0.4 L$. Storage rings should be designed with the optimum condition for the undulator brightness in mind. However, the minimum is a broad one,¹⁰ and the brightness reduction away from the optimum β_x and β_y is not severe. For reasonable β_x and β_y , the undulator radiation is essentially coherent transversely if $\epsilon_x, \epsilon_y \lesssim \lambda/4\pi$.

5. Undulators and Wigglers for the 1–2 GeV Light Source at Berkeley

There are several proposals for next-generation synchrotron radiation facilities.^{1,2,3,23} These are all based on low-emittance (less than 10^{-8} m-rad), high-current (several hundred milliamperes) electron or positron storage rings, and are optimized for undulator operation to produce high-brightness radiation. Of these the 5–7 GeV machines are optimum for hard x-rays, and the 1–2 GeV machines for the VUV and the soft x-ray spectral regions. Here we describe the undulators and wigglers performances for one of the latter machines, the 1–2 GeV Light Source proposed by Lawrence Berkeley Laboratory.¹ The electron parameters of the Light Source relevant to our discussion here are electron energy = 1.5 GeV, beam current (average) = 400 mA, $\epsilon_x = 4 \times 10^{-9}$ m-rad, and $\epsilon_y = 0.1 \times \epsilon_x$.

The spectral brightness for four possible undulators and a wiggler are shown in Fig. 3. For this calculation, the simple approximation based on the Gaussian shape¹¹ is used. The coherence will be characterized by the coherent power P_{coh} which is defined to be the portion of the total power that is transversely coherent and that has a coherence length of 1 micron. In practical units, this becomes

$$P_{coh} [\text{watts}] = 7.63 \times 10^{-23} \times \mathcal{R}(0,0)/\epsilon^2 [\text{keV}]^2, \quad (33)$$

where ϵ is the photon energy and \mathcal{R} is in units of photons per sec per $(\text{mm})^2$ per $(\text{mrad})^2$ per 0.1% bandwidth. Figure 4 gives the coherent power corresponding to Fig. (3).

6. From Undulators to High-Gain Free Electron Lasers

In simple undulators discussed so far, electrons, which are initially uncorrelated, remain essentially uncorrelated as the electron bunch moves through the undulator. The radiation emitted in this case, called the undulator radiation, is analogous to the spontaneous emission in atomic systems. As the number of the undulator periods, N , increases, the cumulative effects of the radiation-electron beam interaction could lead to a density modulation in the electron beam and an exponential amplification of the undulator radiation. When this happens, the radiation become fully coherent transversely, and the transverse profile is given by a mode function independent of z . Undulators operating in this regime will be called the high-gain FELs. The radiation emitted in this case will be called self-amplified spontaneous emission (SASE) by analogy with laser terminology.

The high-gain FELs operating in the SASE mode do not require the use of high-reflectivity mirrors to form optical cavities. Thus, they are promising alternatives to the usual FELs as generators of intense, coherent radiation at wavelengths shorter than 1000 Å. At microwave

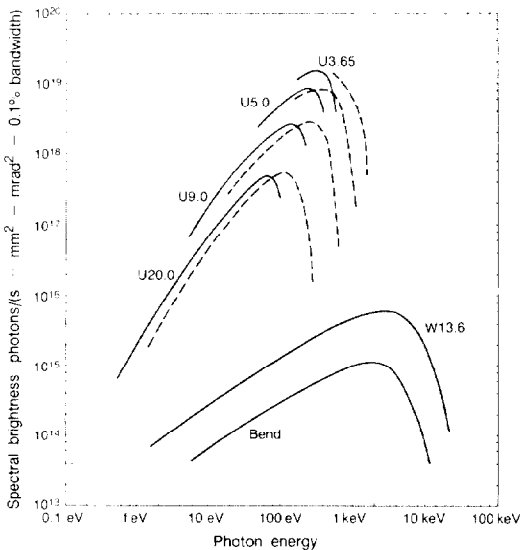


Fig. 3. The spectral brightness from the proposed 1–2 GeV Light Source at Berkeley.¹ The insertion devices are labeled by a capital letter (U = undulator, W = wiggler) followed by the period length in cm. For undulators, solid line represents the fundamental and the dashed lines the third harmonic radiation.

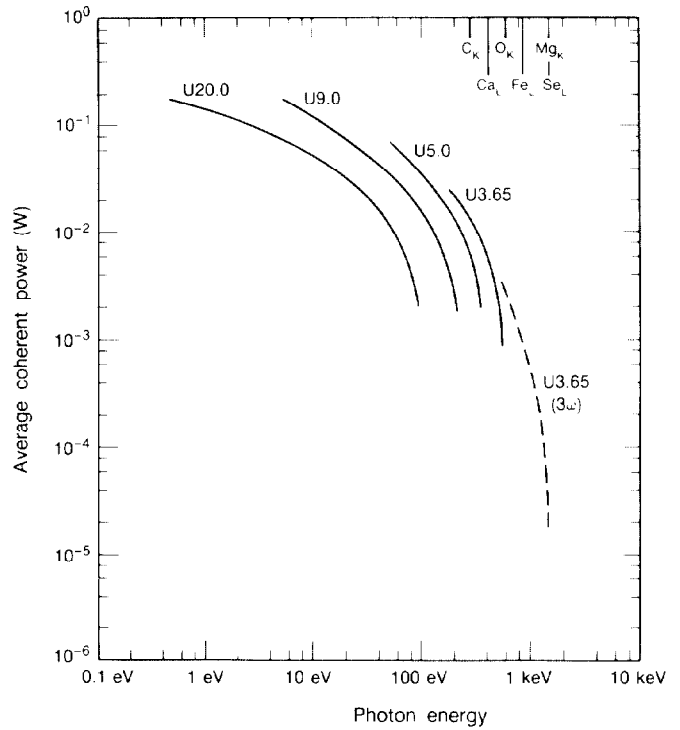


Fig. 4. The average coherent power from undulators for the 1–2 GeV Light Source. The solid and the dashed lines are for the fundamental and the third harmonic radiation, respectively.

wavelengths, the principle of SASE has been experimentally confirmed at Lawrence Livermore National Laboratory.²⁴

(a) Characteristics

The radiation characteristics of high-gain FELs have been studied with various degrees of sophistication.^{15,25–29} Here, we summarize the results of the recent analysis based on the three-dimensional Maxwell-Klimontovich equations.¹⁵

An important parameter characterizing high-gain FELs is the following dimensionless quantity:²⁵

$$\rho = \left[\frac{e j K^2 |JJ|^2 \lambda_u^2}{32 (2\pi)^2 \gamma_0^3 m c^3 \epsilon_0} \right]^{1/3} \quad (34)$$

where j is the beam current density and $|JJ|$ is the Bessel function factor defined in Eq. (20). For cases considered here, ρ is typically of order 10^{-3} .

Figure 5 summarizes the evolution of radiation characteristics from simple undulators to SASE. For $\rho N \leq 0.1$, the radiation is an incoherent superposition of radiation from individual electrons and is referred to as undulator radiation. It is partially coherent transversely due to finite electron beam emittances. The bandwidth $\Delta\lambda/\lambda$ is about $1/N$. For larger N but with $\rho N \leq 1$, the FEL interaction causes modulation in the correlation of the electrons, resulting in enhanced radiation intensity and coherence. Barring certain degenerate situations, the radiation amplitude is dominated by a single mode which grows exponentially, and is fully coherent transversely. The relative bandwidth in this exponentially growing regime is smaller than that of the undulator radiation by a factor $\sqrt{\rho N}$. The emitted power is given by

$$P_{SASE} = \rho P_{beam} g_s e' / N \ell_c, \quad (35)$$

where P_{beam} is the kinetic power contained in the electron beam, g_s is a constant of order unity, $\tau = 8\pi\mu_I \rho N$, μ_I is the imaginary part of the solution of a dispersion relation¹⁵ ($\mu_I = \sqrt{3}/2$ for ideal case), $N \ell_c$ = the number of electron in one coherence length $\ell_c = \lambda^2/\Delta\lambda$. Finally, the exponential growth stops when $\rho N \sim 1$ due to the increased momentum spread induced by the FEL interaction. The radiation power in this “saturated” regime is about ρP_{beam} .

High-gain FELs can also be used in an amplifier mode if coherent input radiation is available at the desired wavelengths. The coherence properties of the emitted radiation in this mode would be the same as those of the input.

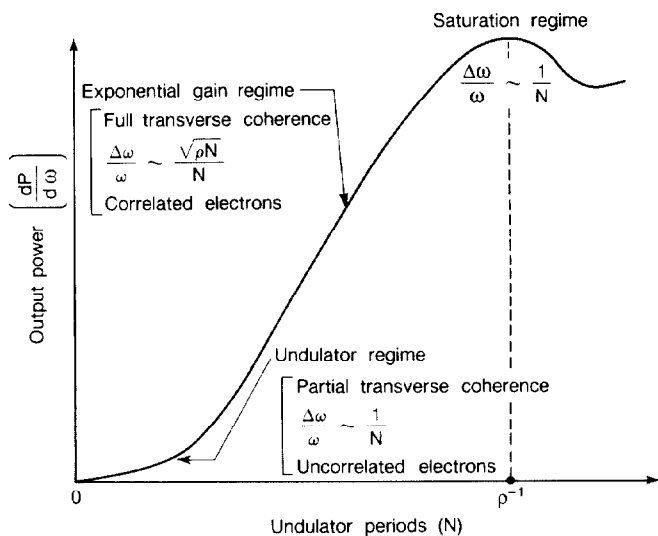


Fig. 5. A schematic illustration of SASE as it grows from noise to saturation as N increases.

(b) A High-Gain FEL in a Bypass of a Storage Ring

Modern storage rings provide the high-density electron beams required for high-gain FEL operation. For efficient interaction, the undulator must be long and have a narrow gap. Such a device, if placed in a normal section of a storage ring, would severely limit the acceptance of the ring and thus reduce the beam lifetime due to scattering with the residual gas. Moreover, the interaction of the beam with an FEL undulator is disruptive to the beam itself in terms of energy loss and increased momentum spread. To avoid these problems, the undulator can be placed in a special bypass section and the high-gain FEL is operated with a repetition rate of the synchrotron radiation damping.⁷

A feasibility study of a optimized storage ring for a high gain FEL operating at 400 Å was recently carried out at Lawrence Berkeley Laboratory.^{8,30} Important aspects of storage ring issues, such as collective instabilities and lattice optimization, bypass considerations, and operational requirements were studied. The storage ring for the Light Source discussed in Section 5 is not optimized for high-gain FELs, but could still provide significant performance when the beam energy is lowered to 750-MeV. Table 1 gives the electron beam parameters for 750-MeV operation and possible undulator parameters for 400 Å radiation.³¹ The expected amplification factors (for the amplifier mode) and the SASE power is shown for different undulator lengths in Table 2. The laser saturates for a 45-m undulator, and generates 10 MW of SASE power. However, the maximum length of the undulator in a bypass that can be fitted inside the storage ring is 20 m, for which the SASE power is only 0.8 kW. To reach saturation in a 20-m undulator, we can install two low-reflectivity mirrors at each end of the undulator, and run the storage ring with a few electron bunches separated by twice the distance between mirrors. Mirrors at these wavelengths could be made from multilayer materials. Assuming a moderate reflectivity of 30%, saturated laser operation is possible with three bunches stored in the ring.

Table 1. Electron-beam and undulator parameters for a 400 Å high-gain FEL.

Electron energy	750 MeV
Horizontal emittance	3.5×10^{-9} m-rad
Vertical emittance	3.5×10^{-10} m-rad
Peak current	20 A
Momentum spread	0.1%
Undulator period	2.34 cm
K (peak)	3.65
Magnet gap	3.5 cm
ρ	8.8×10^{-4}

Table 2. Performance of a high-gain FEL operating in a storage ring with the parameters of the LBL Light Source

Length of the Undulator	Amplification	SASE Power
20 m	1300	0.8 kW
25 m	8000	5.0 kW
45 m	10^7	10.0 MW

References

- [1] Lawrence Berkeley Laboratory Report, 1-2 GeV Synchrotron Radiation Source, 1986, PUB-5172 Rev.
- [2] Y. L. Cho, GXS: Status and Overview of Synchrotron X-Ray Source at Argonne, these proceedings.
- [3] J. L. Laclare, Overview of the European Synchrotron Light Source, these proceedings.
- [4] D. T. Atwood and K-J. Kim, Nucl. Instr. and Meth., A246, p. 86, 1988.
- [5] J. M. J. Madey, J. Appl. Phys., 42, p. 1906, 1971.
- [6] See, for example, papers in the *Proceedings of the 7th Int. Conf. on FELs*, 1985, Nucl. Instr. and Meth., A250, 1986.
- [7] J. B. Murphy and C. Pellegrini, Nucl. Instr. Meth., A237, p. 159, 1985.
- [8] K-J. Kim, J. J. Bisognano, A. A. Garren, K. Halbach, and J.M. Peterson, Nucl. Instr. and Meth., A239, p. 54, 1985.
- [9] D. F. Alferov, Y. A. Bashmakov, and E. G. Bessonov, Sov. Phys. Tech. Phys., 18, p. 1336, 1974.
- [10] S. Krinsky, IEEE Trans. Nucl. Sci., NS-30, p. 3078, 1983.
- [11] K-J. Kim, Nucl. Instr. Meth., A246, p. 71, 1986.
- [12] R. Coisson and R. P. Walker, *SPIE Proceedings*, vol. 582, p. 24, 1986.
- [13] W. Wigner, Phys. Rev., 40, p. 749, 1932.
- [14] K-J. Kim, *SPIE Proceedings*, vol. 582, p. 2, 1986.
- [15] K-J. Kim, Phys. Rev. Lett., 57, p. 1871, 1986.
- [16] M. Born and E. Wolf, *Principle of Optics*, 6th ed., New York: Pergamon Press, 1980, ch. 4.
- [17] See, for example, A. P. Banford, *The Transport of Charged Particle Beams*, London: E & F.N. Spon Limited, 1962.
- [18] See, for example, A. Yariv, *Quantum Electronics*. New York: John Wiley & Sons, 1975.
- [19] See, for example, J. D. Jackson, *Classical Electrodynamics*. New York: John Wiley & Sons, 1962.
- [20] See, for example, J. W. Goodman, *Statistical Optics*. New York: John Wiley & Sons, 1985, ch. 5.
- [21] We thank K. Halbach for this technique.
- [22] K-J. Kim, "Brightness and Coherence of Synchrotron Radiation and High-Gain FELs," paper presented at SR-86, Novosibirsk, USSR, LBL-22317, 1986.
- [23] H. Winnick, "Status of Synchrotron Radiation Facilities Outside the USSR," paper presented at SR-86, Novosibirsk, USSR, 1986.
- [24] T. J. Orzechowski, et al., Phys. Rev. Lett., 54, p. 889, 1985.
- [25] B. Bonifacio, N. Narducci, and C. Pellegrini, Opt. Comm., 50, p. 373, 1984.
- [26] K-J. Kim, Nucl. Instr. Meth., A250, p. 396, 1986.
- [27] J. M. Wang and L. H. Yu, Nucl. Instr. Meth., A250, p. 484, 1986.
- [28] L. H. Yu and S. Krinsky, *AIP Conference Proceedings*, No. 147, 1986, p. 299.
- [29] S. Krinsky and L. H. Yu, "Output Power in Guided Modes for Amplified Spontaneous Emission in Single Pass FEL," BNL 38962, 1986.
- [30] J. J. Bisognano, et al., Particle Accelerators, 18, p. 223, 1986.
- [31] The calculation is due to M. Zisman.